Kinetics of martensitic transitions in Cu-Al-Mn under thermal cycling: Analysis at multiple length scales

Francisco-José Pérez-Reche, Marcelo Stipcich,* Eduard Vives, Lluís Mañosa, and Antoni Planes
Departament d'Estructura i Constituents de la Matèria, Facultat de Física, Universitat de Barcelona, Diagonal, 647, E-08028 Barcelona, Catalonia, Spain

Michel Morin
Groupe d'Etudes de Métallurgie Physique et Physique des Matériaux, INSA Lyon 20, Avenue A.Einstein, 69621 Villeurbanne, France
(Received 12 August 2003; published 9 February 2004)

In this paper we study the evolution of the kinetic features of the martensitic transition in a Cu-Al-Mn single crystal under thermal cycling. The use of several experimental techniques including optical microscopy, calorimetry, and acoustic emission, has enabled us to perform an analysis at multiple scales. In particular, we have focused on the analysis of avalanche events (associated with the nucleation and growth of martensitic domains), which occur during the transition. There are significant differences between the kinetics at large and small length scales. On the one hand, at small length scales, small avalanche events tend to sum to give new larger events in subsequent loops. On the other hand, at large length scales the large domains tend to split into smaller ones on thermal cycling. We suggest that such different behavior is the necessary ingredient that leads the system to the final critical state corresponding to a power-law distribution of avalanches.

DOI: 10.1103/PhysRevB.69.064101 PACS number(s): 64.60.My, 81.30.Kf

I. INTRODUCTION

Many different systems undergoing a first-order phase transition need to be driven by an external field for the transition to occur. The process usually takes place through a sequence of discontinuous steps or avalanches of the order parameter, which reflect the fact that the system jumps from one metastable free energy minimum towards another minimum with an associated energy dissipation and is responsible for the hysteresis observed in these transitions. Typically, the metastable minima are separated by very high or even diverging energy barriers and, therefore, the transition kinetics is not dominated by thermal fluctuations. The configuration of metastable minima determines a complex free-energy landscape which is at the origin of the properties of these systems: the noisy nature of the response to the driving field, and mesoscale phase separation reflected in a polyvariant structure.[1] Martensitic materials are typical examples of this type of systems. In these materials avalanches are related to sudden changes in the local strain field. These changes give rise to acoustic emission (AE) waves in the range from kHz to MHz, characteristic of martensitic transitions.[2] The study of these transient acoustic waves is of great interest since they provide relevant information related to the relaxation kinetics from one metastable state to another. It is worth noting that the AE in martensitic (elastic) systems is the analog of Barkhausen noise in magnetic materials, which is associated with sudden changes of the local magnetization. Furthermore, the phenomenology is typical of a broad class of systems characterized by a complex free-energy landscape with many metastable local minima, a consequence of the existence of disorder and also of long-range (anisotropic) interactions which are operative during the transition. Besides magnetic and elastic systems, other examples are ferroelectrics,[3] superconductors,[4] etc. The long-range interactions are the essential feature which are necessary to understand the formation of the polyvariant structures in these types of materials.

In elastic systems, the physical cause of long-range interactions is the coherency strain between the parent and martensitic phases,[5] which can be conveniently expressed taking into account the coupling between the strain tensor components resulting from elastic compatibility constraints.[6] Moreover, it has recently been shown that competition between interactions at different length scales is the relevant ingredient for the formation of a metastable mesostructure.[7,8] Disorder is, however, important for the nucleation of the product phase and thus in determining the specific path followed by the system at the transformation.

An interesting feature regarding AE is the power-law behavior of the distribution of amplitudes and duration of the emitted acoustic signals. This behavior, which is only observed in systems that have been thermally cycled through the transition,[9] has been related to the fact that the transition proceeds without characteristic time and length scales and is the prototypical signature of criticality. This feature is expected to be a consequence of a combined effect of the amount and distribution of disorder and of the long-range interactions that determine the suitable free-energy landscape to enable criticality. Why such a situation is reached after a certain number of cycles through the transition is still not well understood. The study of this problem is the main goal of the present paper.

The study of cycling has been the aim of a large number of works published in the past.[10] These papers essentially focused on the effect of cycling on transition temperatures since reproducibility of thermodynamic properties through cycling is required in order to ensure high efficiency in engineering shape-memory applications. Actually cycling is expected to change both the amount and the properties of disorder in the system. For instance, it is known that thermal cycling results in the creation of crystal defects such as dislocations.[11,12] Any modification in the amount of disorder

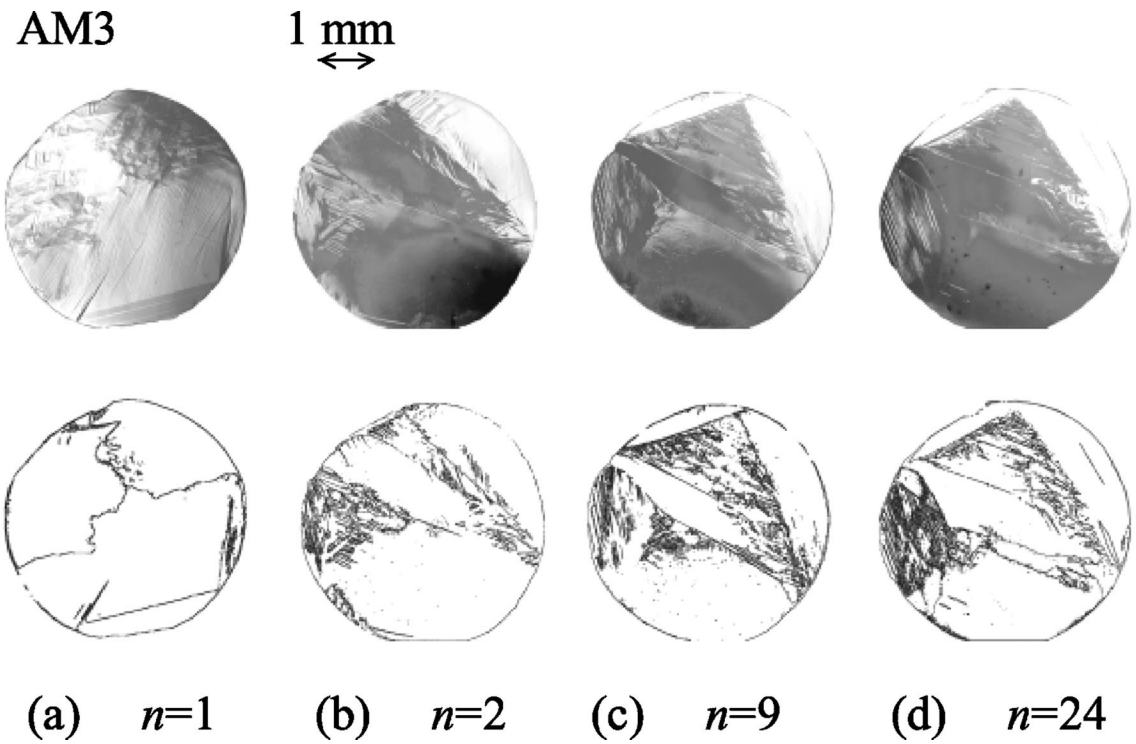

FIG. 1. Micrographs of sample AM3 taken in the martensitic state, at $T=220$ K, after the 1st, 2nd, 9th, and 24th cooling runs. Below each micrograph we show the result of a digital analysis enhancing the boundaries between the different variants.

should be reflected on the characteristics of the AE generated during the transition.

In the present paper we have studied the evolution of the martensitic transition of a Cu-Al-Mn single crystal under thermal cycling. We have combined several experimental techniques in order to analyze the behavior at different length scales.

(i) Calorimetric measurements provide a description of the integrated behavior at a macroscopic scale. In particular, we have measured the evolution with cycling of the transition temperatures, latent heat, entropy change, and dissipated energy.

(ii) Optical microscopy is adequate to characterize the polyvariant structure after each transformation cycle at length scales ranging from cm to μm.

(iii) The detection of AE signals enables one to characterize avalanche events over a broad range of time scales, from microseconds to seconds.

II. EXPERIMENTAL DETAILS

The sample used in the present study was a Cu-Al-Mn single crystal which is a prototypical shape-memory alloy. The master alloy from which the crystal was grown, was prepared by adding appropriate quantities of 99.99% pure Cu, Al, and Mn. The crystal was grown by the Bridgman technique in a quarz crucible in vacuum. It was homogenized at 1073 K for about 48 h, and then left to cool down in air to room temperature. This heat treatment ensures that a metastable β phase (ordered-bcc) is obtained at room temperature. On further cooling, a martensitic transition is observed to a $2H$ structure.

For optical microscopy, calorimetry and AE experiments, slices were cut from the original rod using a low-speed diamond saw. Typical dimensions of the slices were 2-mm thick and 4-mm diameter. In the present paper, the different slices will be denoted by a number that indicates the order in which they were cut, starting from one end of the rod. To remove stresses generated during cutting, all the slices were subjected to a further homogenization at 1073 K for 30 min and then left to cool down in air to room temperature. All the samples were then annealed at room temperature for about 48 h, in order to be sure that all reordering processes were finished, and that the vacancy concentration reached its equilibrium value.[13] The composition of all slices was checked by energy dispersive x-ray analysis system (EDAX). Deviations from the average value Cu 71.7 at. %, Al 20.1 at. %, and Mn 8.2 at. % were less than 0.5 at. %.

Samples for optical microscopy were first mechanically polished with fine grinding paper, followed by final polishing with 3-μm diamond powder. Optical observations were performed using an optical microscope equipped with a charge-coupled-device video camera and a heating/cooling stage, which enabled the transformation of the samples to be monitored *in situ*. Typical heating/cooling rates were $\dot{T}=10$ K/min.

Calorimetric experiments were performed using a high-sensitive differential scanning calorimeter, specifically designed for the study of solid-solid phase transitions.[14] Typical heating/cooling rates were about $\dot{T}=0.5$ K/min.

AE signals were recorded during heating and cooling ramps at rates of 0.1 K/min. We used a piezoelectric transducer working in a band centered at 1 MHz, acoustically

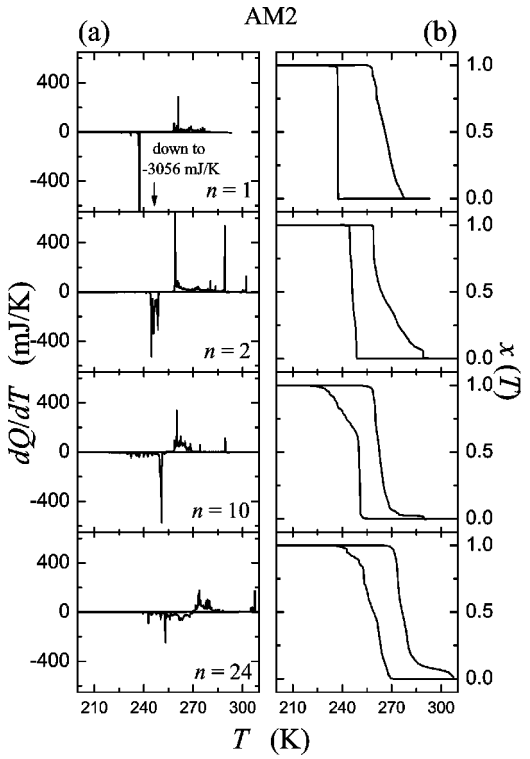

FIG. 2. Thermograms (a) and hysteresis loops (b) for selected cycles through the forward and reverse martensitic transitions of sample AM2.

coupled to the surface of the sample. After being amplified (gain of 62 dB) the AE signal was processed simultaneously by two different methods. On the one hand, bursts with amplitudes exceeding a fixed threshold were stored using a digitizing oscilloscope which is capable of recording 10^4 AE pulses (1000 points per signal at 1 MHz) during the martensitic transition. On the other hand, the signal was input into a ring-down frequencymeter which renders the count rate $\dot{N} = dN/dt$ (the number of signals recorded during a time interval $\Delta t = 1$ s). Notice that this parameter gives information of integrated measurements on a long time scale.

III. EXPERIMENTAL RESULTS

A. Optical microscopy

Several samples were subjected to repeated cycling through the martensitic transition (from room temperature down to 220 K). During cycling, the evolution of the surface of the samples was recorded.[15] The following qualitative information can be extracted from the analysis of the recordings.

(i) The kinetics of the transformation were different for each sample. Furthermore, the final microstructure was different.

(ii) Although they had different kinetics, the samples exhibited the same tendency towards a reproducible transition on cylcing. That is, for the first cycles, both the kinetics and microstructure of one cycle were not similar to the previous cycle, but upon repeated cycling, the kinetics and microstructure became similar from one cycle to the next. This final reproducible pattern differs from one sample to another.

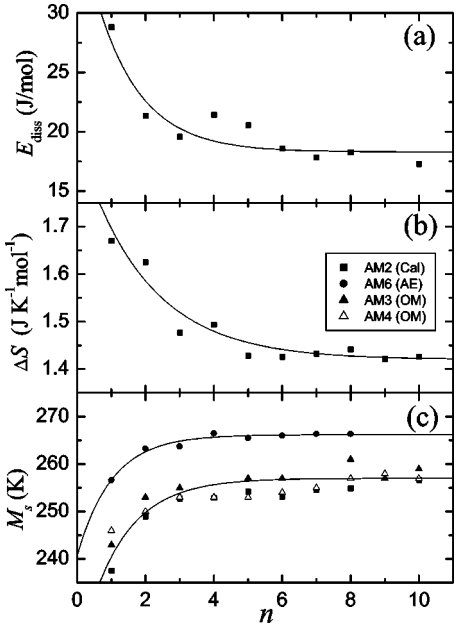

FIG. 3. (a) Dissipated energy, (b) entropy change, and (c) martensite starting temperature as a function of cycling, for sample AM2. In (c), the values obtained from optical microscopy in samples AM3 (solid triangles) and AM4 (open triangles) are also shown.

As a typical example of the behavior described above, Fig. 1 illustrates the evolution of the microstructure corresponding to sample AM3. Above we show the pictures of the final microstructure (at 220 K) observed after the 1st, 2nd,

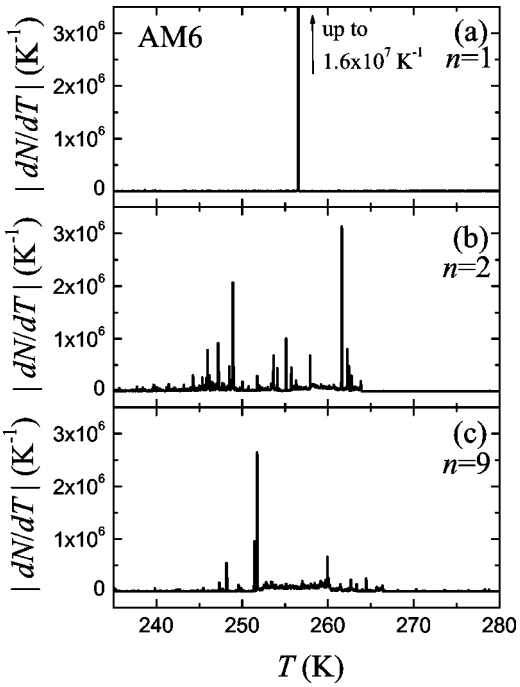

FIG. 4. Counting rate dN/dT as a function of temperature for the first, second, and ninth cooling runs of sample AM6.

9th, and 24th cycles. Below, we present the pictures resulting from a digital analysis. The boundaries between different variants are more clearly seen. The number of martensitic variants increases during the first few cycles, and evolves towards a reproducible pattern.

It is worth remarking that it is difficult to obtain systematic results from the optical microscopy measurements. In particular we observed that when the sample is able to find a transforming path ending in an almost single variant martensite, such a path has a tendency to become more reproducible in further cycles. Nevertheless, the confirmation of this tendency would require a systematic study of a large number of samples, since such a final single variant martensite is obtained with very low probability.

B. Calorimetric results

The effect of thermal cycling on sample AM2 was studied by calorimetry. Figure 2(a) shows the thermal curves (thermograms) recorded during cooling and heating runs for cycles 1, 2, 10, and 24. There is a clear evolution of the shape of the thermograms under cycling which reflects the change in microstructure.

The entropy change (ΔS) at the martensitic transition is obtained from the thermograms, after a proper correction from the baseline, as

$$\Delta S = \int_{T_i}^{T_f} \frac{1}{T} \frac{dQ}{dT} dT, \tag{1}$$

where T_i is a temperature above (below) the starting transition temperature on cooling (heating) and T_f is a temperature below (above) the finishing transition temperature on cooling (heating). It is also possible to compute the transformed fraction x as

$$x(T) = \frac{1}{\Delta S} \int_{T_i}^{T} \frac{1}{T} \frac{dQ}{dT} dT, \tag{2}$$

which enables one to obtain the hysteresis loops. In Fig. 2(b) we present these loops for cycles 1, 2, 10, and 24. As the number of cycles increases, the loop becomes less sharper, and the area enclosed within the loop diminishes. It is worth noting that this area is related to the energy dissipated in a complete loop as

$$E_{diss} \simeq \Delta S \oint x dT. \tag{3}$$

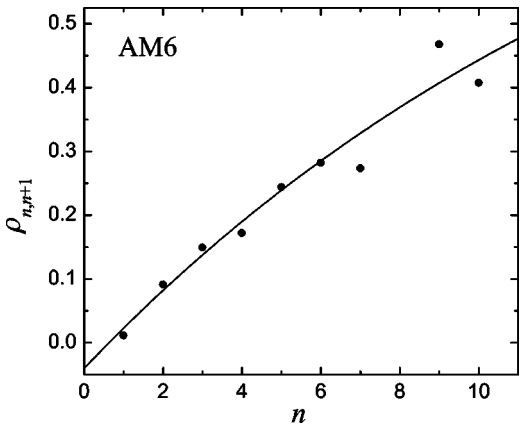

FIG. 5. Correlation function between the reduced AE activity of consecutive cycles, as a function of cycle number, for sample AM6.

Figure 3(a) shows the dissipated energy as a function of the number of cycles. A clear decrease is observed upon repeated cycling. The evolution of ΔS (averaged over heating and cooling runs) as a function of cycling is shown in Fig. 3(b). A significant decrease is also observed for the first cycles. Upon thermal cycling both E_{diss} and ΔS tend to a constant value. Figure 3(c) shows the evolution of the martensitic starting temperature (determined from the thermograms), as a function of cycle number, for sample AM2. We have also included the values determined from optical microscopy in samples AM3 and AM4 and from AE in sample AM6. In the early stages of cycling, M_s increases with the number of cycles for all samples, and reaches a constant value at about eight to ten cycles. It is worth remarking that although the microstructure of all samples is different, this increasing behavior exhibited by the transition temperature is sample independent, thus showing that this is a general phenomenon associated with thermal cycling.

C. Acoustic emission results

The effect of thermal cycling on the AE generated during the martensitic transition was investigated for two different approaches in sample AM6: (i) analyzing the counting rate changes and (ii) examining the evolution in the distribution of amplitudes of AE signals.

Figure 4 shows the reduced AE count rate $[r(t) = dN/dT = \dot{N}/\dot{T}]$ recorded during cooling runs for cycles 1 (a), 2 (b), and 9 (c). The pattern differs significantly from one cycle to the other. A quantitative evaluation of the similarity in the AE pattern is achieved by computing the correlation function between the reduced AE activity of two consecutive cycles as

$$\rho_{n,n+1} = \frac{\int_{T_i}^{T_f} r_n(T) r_{n+1}(T) dT - \int_{T_i}^{T_f} r_n(T) dT \int_{T_i}^{T_f} r_{n+1}(T') dT'}{\sqrt{\left[\int_{T_i}^{T_f} r_n^2(T) dT - \left(\int_{T_i}^{T_f} r_n(T) dT \right)^2 \right] \left[\int_{T_i}^{T_f} r_{n+1}^2(T) dT - \left(\int_{T_i}^{T_f} r_{n+1}(T) dT \right)^2 \right]}}, \tag{4}$$

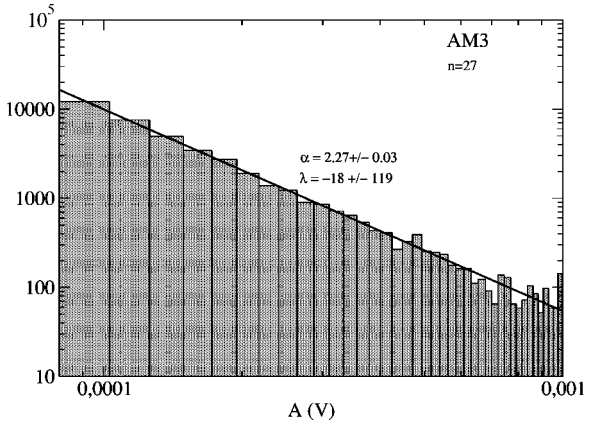

FIG. 6. Histogram corresponding to the distribution of amplitudes of AE signals recorded during the 27th cooling run of sample AM3. The continuous line shows the fitted function defined in Eq. (5) with $\lambda=-18$ and $\alpha=2.27$.

where $r_n(T)\equiv(\dot{N}/\dot{T})_n(T)$ for cooling corresponding to the nth cycle. The value of this function quantifies how much the reduced acoustic activity as a function of temperature in the nth cycle resembles that of the $(n+1)$th. When r_n is very similar to r_{n+1}, $\rho_{n,n+1}$ is close to unity.

The correlation function between the nth and $(n+1)$th transformation versus the cycle number n is presented in Fig. 5. A clear increase in the correlation is observed with cycling which indicates that the transition becomes progressively more reproducible. Although the value of $\rho_{n,n+1}$ is still far from $\rho_{n,n+1}=1$, the clear tendency to increase indicates that after a large number of cycles the pattern will become reproducible.

From the study of the individual AE signals recorded on a digitizing oscilloscope, it is possible to perform a statistical analysis of the distribution of amplitudes. An example of the AE amplitude distribution obtained for the 27th cooling run in sample AM3 is shown in Fig. 6. It has been established[9,16] that for martensitic transitions, the AE amplitude distributions can be analyzed using the following probability distribution with two free parameters (λ and α):

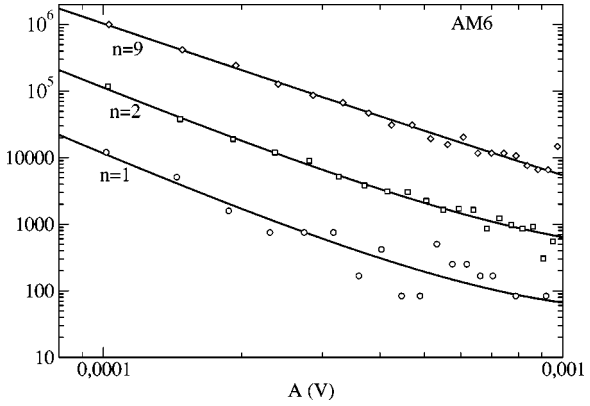

FIG. 7. Distribution of amplitudes of the AE signals recorded during the first, second, and ninth cooling runs of sample AM6. Symbols correspond to the height of the histogram bins and lines stand for the fitted functions. The distributions corresponding to $n=2$ and $n=9$ have been shifted upwards for clarity.

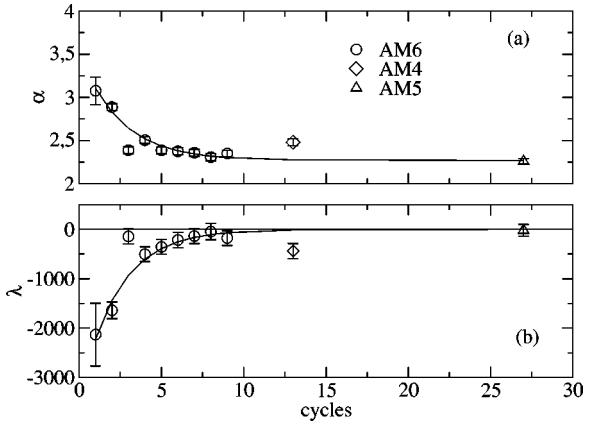

FIG. 8. The exponent α (a) and the factor λ (b) obtained for cooling runs of sample AM6 as a function of the cycle number. The values obtained in the 13th cycle of sample AM4 (diamond) and the 27th cycle of sample AM3 (triangle) are also shown.

$$p(A)=\frac{\exp(-\lambda A)A^{-\alpha}}{\int_{A_{min}}^{A_{max}}\exp(-\lambda A)A^{-\alpha}}, \tag{5}$$

where A is the amplitude of the AE signal. The parameter λ measures the deviation from the power-law behavior. For $\lambda=0$, the distribution is a pure power law, while it is subcritical for $\lambda>0$ and supercritical for $\lambda<0$. $A_{min}=8\times10^{-5}$ V and $A_{max}=10^{-3}$ V are the limits of the experimental window imposed by the detection setup.

We have estimated the exponent α and the parameter λ using the maximum likelihood method.[17] This method is the most reliable one since it does not involve the computation of histograms, which normally depend on the binning choice.

In Fig. 6 we present the results obtained from the analysis of a set of $\sim7\times10^3$ signals corresponding to cycle 27 of the sample AM3. We present a normalized histogram and the fit (continuous line) of Eq. (5). In this case the AE avalanche distribution is almost power law with $\alpha=2.26\pm0.03$ and a value of λ which is compatible with $\lambda=0$. This result is in

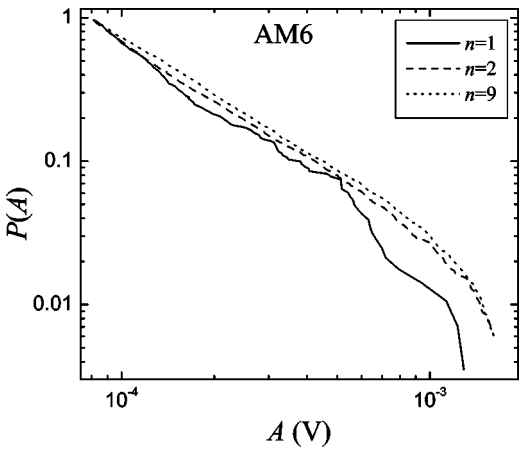

FIG. 9. Cumulative distribution of amplitudes of the AE signals recorded during the first, second, and ninth (from top to bottom) cooling runs of sample AM6.

good agreement with the results previously published[16] corresponding to samples with a large number of cycles and which transform to the same martensitic structure.

Figure 7 shows the fits of the distributions corresponding to cycles 1, 2, and 9 of the sample AM6. The comparison of the different plots reveals that during the first loops there is an evolution of the distribution of avalanches.

Figure 8 shows the actual evolution of the fitted exponent α and the parameter λ with cycling. The values for the highly cycled samples AM4 and AM3 are also shown. On thermal cycling, the exponent α decreases towards a stable value, and the factor λ tends to zero.

This evolution is more clearly seen by plotting the cumulative distribution function $P(A)$, defined as the ratio between the number of signals with amplitude greater than A over the total number of recorded signals (per half loop). The change of $P(A)$ with cycling is plotted in Fig. 9. It is clear that the relative number of signals with a large amplitude increases with cycling compared with the number of signals with a small amplitude.

IV. DISCUSSION

In the present paper we have studied the influence of thermal cycling on the martensitic transition of a Cu-Al-Mn shape-memory alloy. A significant evolution in the kinetics of the transformation has been found during thermal cycling. Such an evolution can be understood as a learning process in which the system seeks an optimal path in the space of internal variables of the system that connects the parent and martensitic phases. This optimal path tends to avoid high-energy barriers which separate local metastable states. In such a way, increasing thermal cycling reduces metastability. Clear evidence of this effect is the reduction of the dissipated energy as shown in Fig. 3(a). After the learning period, a stationary state is reached for which the dissipated energy is a minimum according to Prigogine's theorem,[18] and at this point the transition is much more reproducible from cycle to cycle.

From the small-scale analysis of the distribution of AE signals, it is seen that the relative number of small avalanches decreases with respect to the number of larger avalanches. This is reflected by the decrease of the exponent α during the first thermal cycles (Fig. 8), and also in the cumulative distribution in Fig. 9. This behavior has been observed in all the studied samples. Moreover, the tendency for the distribution of avalanches to evolve towards a power law should be pointed out, as is revealed by the evolution of λ in Fig. 8(b). The stationary value of α is in agreement with the previous estimations[16] for alloys transforming to the $2H$ structure, thus supporting the idea of ''universality'' for this α exponent after the ''learning'' period.

In contrast, the macroscopic measurements suggest that thermal cycling favors the rupture of large variants into smaller ones. This effect is seen by both optical microscopy and by the evolution of the thermograms (Fig. 2) and counting rate (Fig. 4), which become smoother with increasing cycling. In general, the first loop essentially causes a single large event that splits into many smaller events after a few cycles. A more quantitative proof of this result can be achieved by performing an analysis of the distribution of the height of the peaks in the counting rate. A statistical analysis of the height of the different peaks in dN/dT (see Fig. 4) can be performed by defining a proper threshold (background). The histograms resulting from this analysis are shown in Fig. 10. The comparison of the histograms corresponding to different cycles reveals that large peaks tend to split into smaller ones. A similar analysis can be performed on the thermograms in Fig. 2, rendering similar qualitative results. The tendency for the histograms in Fig. 10 to become a power law with cycling should again be pointed out. The fitted exponent is 2.7 ± 0.4. The numerical value is very close to that found from the small-scale analysis of AE signals. At present we cannot give an explanation for such a coincidence, since we cannot foresee any direct relationship (proportionality) between the two different physical quantities measured.

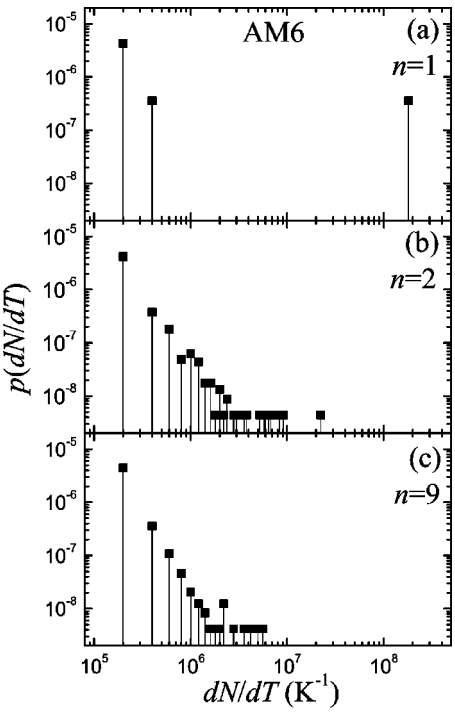

FIG. 10. Histograms corresponding to the peak height distribution of the AE counting rate curves of Fig. 4 for cycles $n=1$, $n=2$, and $n=9$.

This tendency for the large variants to split into smaller ones also explains the increase of the transition temperature with cycling shown in Fig. 3(b). Note that M_s is measured by either calorimetry or AE ring down counting as the temperature at which the first event is resolved. If the transition path splits into a larger number of steps, it is more likely to detect events at higher temperatures (with a lower degree of metastability) on cooling.

The combination of the opposing behavior found at microscopic and macroscopic scales seems to be responsible for the final power-law distribution of events characteristic of these materials. Corroboration of this point will require further analysis and the development of a statistical model. We are, at present, working along these lines and the results will

be presented in a future work.

Finally, we would like to comment on the connections between the experimental observations and related published theoretical approaches. First of all our results are in partial agreement with the behavior of the three-dimensional random-field Ising model (3D-RFIM) with metastable dynamics proposed several years ago as a prototype for the evolution with disorder of the hysteresis in athermal systems.[19] In this model, the disorder is controlled by a scalar variable σ which accounts for the width of the Gaussian distribution of quenched local random fields. The decrease in dissipation that we have demonstrated in martensitic systems, is also obtained in the 3D-RFIM when σ increases. Moreover, the distribution of avalanches evolves from a supercritical ($\lambda<0$) towards a power law ($\lambda=0$) when σ increases towards the critical value σ_c. At this critical point the distribution of avalanche sizes is characterized by an exponent which is supposed to be universal.

Second, our results are also in agreement with those reported more recently from a model for the AE generated during martensitic transitions proposed by Ananthakrishna and collaborators.[20,21] They proposed a 2D model based on a free-energy functional which incorporates (i) an anisotropic effective long-range term compatible with the symmetry of the system that describes the strain-strain interaction and (ii) an inhomogeneous stress field with a Gaussian distribution which is adequate to mimic the nucleation of the martensitic phase in the vicinity of lattice defects. The long-range term is included following the procedure proposed in, Ref. 22 but without properly taking into account elastic compatibility constraints. Dissipation is included by means of a Rayleigh dissipative functional following the ideas first introduced by Bales and Gooding.[23] They state that transformation occurs through energy bursts which are identified with the AE signals. They also found that the size and duration distribution of these transient signals were power law. The striking feature is that the size exponent agrees quite well with the stationary value reported in the present paper. Moreover, the model shows that cycling evolution is mediated by strain-strain long-range interactions. This is obtained by partial cycling through the transition. The essential point is that the martensite remaining in the system, when the temperature is reversed in the heating process, plays an essential role in establishing the ''memory'' from one cycle to the next. Actually, the experimental situation is different. Cycles are performed so that the reverse transition on heating is fully completed. In this case the memory giving rise to the learning process should be associated with permanent lattice defects created during the transition process and not with the remaining martensite domains. The existence of these defects has been extensively reported by several authors.[11,12] In Cu-Zn-Al they are mainly dislocations with Burgers' vector along $\langle 100 \rangle$ direction, which are known to act as nucleation sites and therefore fix the transition path that the system will follow on subsequent cycles. As regards this point we have checked that all the observed memory effects with cycling in Cu-Al-Mn are erased by means of a high-temperature ($\sim$1000 K) heat treatment.

ACKNOWLEDGMENTS

The authors acknowledge Dr. Avadh Saxena for a critical reading of the manuscript. This work has received financial support from CICyT (Project No. MAT2001-3251) and DURSI (Project No. 2001SGR00066). F.J.P.-R. acknowledges financial support from DGICyT. M.S. has received financial support from Secretaría de Estado de Educación y Universidades (Spain).

*Also at Instituto de Fisica de Materiales Tandil (IFIMAT), UNCentro, Pinto 399, 7000 Tandil, Argentina.

[1] S. Kartha, T. Castán, J.A. Krumhansl, and J.P. Sethna, Phys. Rev. Lett. **67**, 3630 (1993).
[2] P.C. Clapp, J. Phys. IV **5**, C8-11 (1995).
[3] B. Tadić, Eur. Phys. J. B **28**, 81 (2002).
[4] W. Wu and P.W. Adams, Phys. Rev. Lett. **74**, 610 (1995).
[5] A.G. Khachaturyan, S.M. Shapiro, and S. Semenovskaya, Phys. Rev. B **43**, 10 832 (1991).
[6] S.R. Shenoy, T. Lookman, A. Saxena, and A.R. Bishop, Phys. Rev. B **60**, R12 537 (1999); T. Lookman, S.R. Shenoy, K.Ø. Rasmussen, A. Saxena, and A.R. Bishop, *ibid.* **67**, 024114 (2003).
[7] J. Schmalian and P.G. Wolynes, Phys. Rev. Lett. **85**, 836 (2000).
[8] H. Westfahl, J. Schmalian, and P.G. Wolynes, Phys. Rev. B **64**, 174203 (2001).
[9] E. Vives, J. Ortín, Ll. Mañosa, I. Ràfols, R. Pérez-Magrané, and A. Planes, Phys. Rev. Lett. **72**, 1694 (1994).
[10] C. Auguet, E. Cesari, and Ll. Mañosa, J. Phys. D **22**, 1712 (1989) and references therein.
[11] D. Ríos-Jara and G. Guénin, Acta Metall. **35**, 109 (1987).
[12] J. Pons, F.C. Lovey, E. Cesari, Acta Metall. Mater. **38**, 2733 (1990).
[13] R. Romero, A. Somoza, Ll. Mañosa, and A. Planes, J. Phys. IV **112**, 499 (2003).
[14] A simplified version of this calorimeter is presented in Ll. Mañosa, M. Bou, C. Calles, and A. Cirera, Am. J. Phys. **64**, 283 (1996).
[15] The complete recording is available from the authors upon request.
[16] Ll. Carrillo, Ll. Mañosa, J. Ortín, A. Planes, and E. Vives, Phys. Rev. Lett. **81**, 1889 (1998).
[17] R. Barlow, *Statistics* (Wiley, New York, 1989).
[18] G. Nicolis and I. Prigogine, *Self-Organization in Non-Equilibrium Systems* (Wiley, New York, 1977).
[19] J.P. Sethna, K. Dahmen, S. Kartha, J.A. Krumhansl, B.W. Roberts, and J.D. Shore, Phys. Rev. Lett. **70**, 3347 (1993); K.A. Dahmen, J.P. Sethna, M. Kuntz, and O. Perković, J. Magn. Magn. Mater. **226-230**, 1287 (2001).
[20] R. Ahluwalia and G. Ananthakrishna, Phys. Rev. Lett. **86**, 4076 (2001).
[21] S. Sreekala and G. Ananthakrishna, Phys. Rev. Lett. **90**, 135501 (2003).
[22] Y. Wang and A.G. Kachaturyan, Acta Mater. **45**, 759 (1997).
[23] G.S. Bales and R.J. Gooding, Phys. Rev. Lett. **67**, 3412 (1991).